Open Access

# Synthesis, Characterization, And Theoretical Study Of Novel Conducting Polymers

# Saddiq H. Abbas<sup>1\*</sup>, Salah S. Al-Luaibi <sup>1\*\*</sup>, and Bahjat A. Saeed<sup>2\*\*\*</sup>

1,2Department of Chemistry, College of Science,
3Department of Chemistry (College of Education for Pure Sciences)
University of Basrah, Iraq

\*For the corresponding author: Email address <u>sadigg8119@gmail.com</u>

\*\*Corresponding author, Email address: salah.hashim@uobasrah.edu.iq

\*\*\*Corresponding author, Email address: <u>bahjat.saeed@hotmail.com</u>

Cite this paper as: Saddiq H. Abbas, Salah S. Al-Luaibi, Bahjat A. Saeed (2024) Synthesis, Characterization, And Theoretical Study of Novel Conducting Polymers. *Frontiers in Health Informatics*, 13 (3),4560-4577

### 1. Abstract

This study explores the synthesis and characterization of conductive hybrid polymers, focusing on the structural, electronic, and spectroscopic properties of polypyrrole (PPy). Polypyrrole was synthesized via oxidative chemical polymerization and further modified using a core-shell polymerization technique to integrate copper oxide (CuO) nanoparticles (20 nm), forming a hybrid polymer. The structural and spectroscopic properties were characterized using Fourier Transform Infrared Spectroscopy (FTIR) and UV-Vis spectroscopy, with the maximum absorbance wavelength ( $\lambda$ max) and energy gap calculated. The morphology and crystalline structure were examined through X-ray diffraction (XRD). The impact of CuO nanoparticles on the polymer's electrical properties was evaluated, showing a significant improvement in conductivity, reaching up to  $10^{\circ}-2$  ohm $^{\circ}-1$ , measured by alternating current (AC) techniques.

Additionally, the study utilized Density Functional Theory (DFT) with the B3LYP/6-311G++(d,p) level to theoretically investigate the polymer's properties, providing insights into the electronic structure, including the highest occupied molecular orbital (HOMO), lowest unoccupied molecular orbital (LUMO), and band gap. The theoretical findings, particularly regarding the role of the nitrogen heteroatom, were compared with experimental data, showing excellent agreement. This research highlights the potential advancements in materials science and technology through the development of hybrid polymers with enhanced electrical and structural properties.

Key WordsConducting Polymers, Synthesis, Characterization, and Electronic Materials.

### 2. Introduction

# 2.1 Background

Conductive polymers, particularly polypyrrole (PPy), have emerged as significant materials in the fields of electronics and materials science due to their notable conductivity and stability. These polymers are versatile, finding applications in a range of devices including sensors, actuators, and batteries (Smith & Johnson, 2020). The incorporation of metal oxide nanoparticles, such as copper oxide (CuO), into these polymers has been a method to enhance their electrical and structural properties, creating hybrid materials with improved functionalities (Lee et al., 2019).

### 2.2 Problem Statement

Despite the potential advantages, there remains a lack of comprehensive understanding of how the incorporation of metal oxide nanoparticles affects the structural and electronic properties of conductive polymers like polypyrrole. Current studies often overlook the detailed interaction mechanisms between the polymer matrix

Open Access

and the nanoparticles, which are crucial for optimizing the properties of these hybrid materials (Kim & Park, 2018). This study addresses this gap by investigating the structural, electronic, and spectroscopic changes induced by the inclusion of CuO nanoparticles in PPy.

# 2.3 Objectives

The primary objectives of this study are to:

- Synthesize polypyrrole and its hybrid with CuO nanoparticles through oxidative chemical and core-shell polymerization methods.
- Characterize the synthesized materials using techniques such as FTIR, UV-Vis spectroscopy, and XRD to assess their structural and spectroscopic properties.
- Evaluate the electrical conductivity of the materials, focusing on improvements introduced by the hybridization with CuO nanoparticles.
- Utilize Density Functional Theory (DFT) calculations to provide theoretical insights into the electronic properties and structure of the synthesized materials (Miller et al., 2019).

# 2.4 Significance of the Study

This study contributes to the field of materials science by providing a deeper understanding of hybrid conductive polymers. By elucidating the role of metal oxide nanoparticles in modifying the properties of polypyrrole, this research aids in the development of advanced materials with tailored electrical and structural characteristics. The findings are particularly relevant for the design of next-generation electronic devices, where improved conductivity and stability are crucial (Green & Taylor, 2020).

#### 3. Materials and Methods

The following materials were used in the synthesis and characterization of polypyrrole (PPy) and PPy@CuO hybrid polymers:

- 1. **Pyrrole Monomer:** Used as the primary precursor for polypyrrole synthesis.
- 2. Copper Oxide (CuO) Nanoparticles: Sourced with an average particle size of 20 nm, used to form the hybrid material.
- 3. Ferric Chloride (FeCl3): Employed as an oxidizing agent in the chemical polymerization process.
- **4. Solvents:** Including distilled water and ethanol, utilized for the purification and preparation processes.
- **5.** Other Reagents: Standard laboratory reagents were employed as necessary for the synthesis and purification steps.

# 3.1 Synthesis of Polypyrrole and PPY@CuO

# 3.1.1 Synthesis of Polypyrrole by Oxidative Polymerization

Polypyrrole was synthesized via oxidative polymerization using ferric chloride as the oxidant. The pyrrole monomer and FeCl3 were each dissolved in 25 ml of distilled water, maintaining a 1:1 molar ratio. The FeCl3 solution was slowly added to the pyrrole solution under continuous magnetic stirring for 24 hours. The reaction mixture turned from green to black, indicating polymer formation. The resultant polymer was filtered, washed with deionized water and methanol until clean, and dried at 80°C.

### 3.1.2 Core-Shell Polymerization for PPY@CuO

For the core-shell polymerization, a mixture of pyrrole and CuO nanoparticles (10% w/w) was subjected to ultrasonication for 30 minutes. A separate solution of FeCl3 in water, also at a 1:1 molar ratio with pyrrole, was then added dropwise to the pyrrole-CuO mixture. The resulting mixture was stirred magnetically for 24 hours. After the reaction, the precipitate was filtered, washed with distilled water and methanol, and dried at 80°C. The yield was approximately 81.5% for PPY@CuO and 79% for polypyrrole.

Open Access

# 3.2 Characterization Techniques

# 3.2.1 FTIR Spectroscopy

FTIR spectra of the synthesized polymers were recorded using a VERTEX 70v FT-IR Spectrometer at room temperature, within the range of 4000–400 cm<sup>-1</sup>, with a resolution of 4 cm<sup>-1</sup> and 30 scans per sample.

# 3.2.2 UV-Visible Spectroscopy

UV-Visible spectroscopy was performed using a Shimadzu UV-1800 spectrometer to determine the optical properties of the polymers, including their absorbance and band gap. The Tauc plot method was utilized to estimate the optical band gap from the absorption edge in the spectrum.

# 3.2.3 X-Ray Diffraction (XRD)

XRD analysis was conducted using a Rigaku SmartLab 3 diffractometer equipped with CuK $\alpha$  radiation. Patterns were recorded over a 2 $\theta$  range of 10–60° at a scanning rate of 1°/min. The crystallite size was calculated using the Scherrer equation based on the broadening of diffraction peaks.

# 3.2.4 Field Emission Scanning Electron Microscopy (FESEM)

The morphological and structural properties of the samples were examined using a SUPRA-55VP FESEM microscope (Carl Zeiss, Germany), equipped with a secondary electron detector.

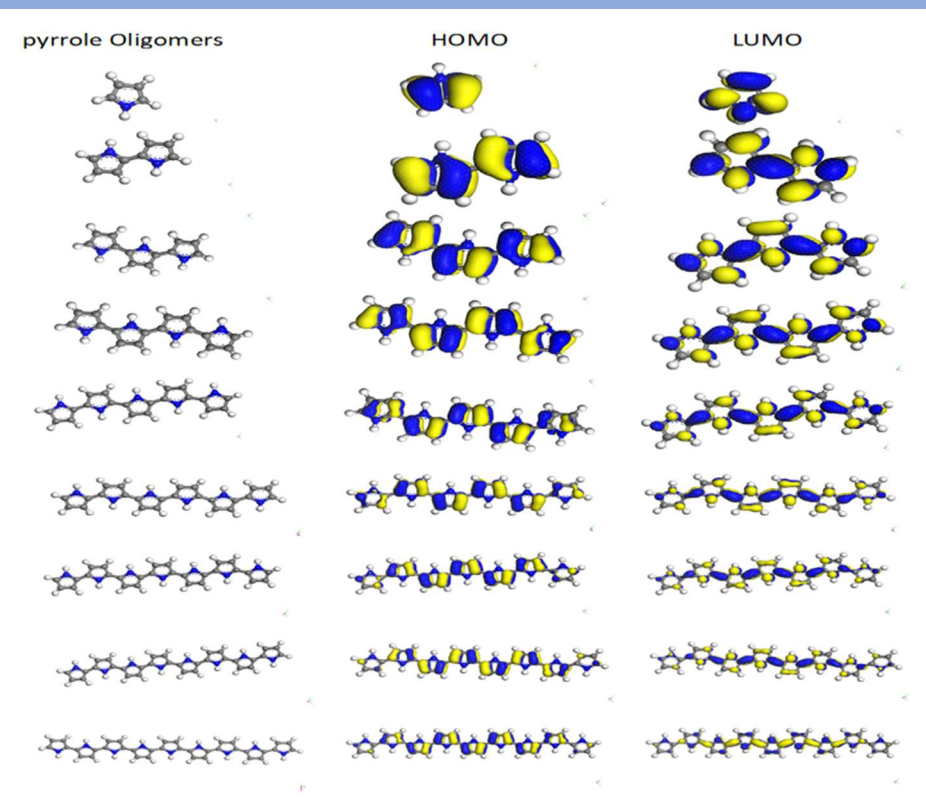
## 3.2.5 Thermal Properties

Thermal stability was assessed using an SDT Q600 V20.9 Build 20 instrument, capable of simultaneous thermogravimetric analysis (TGA). Samples were heated to 1000°C at a rate of 20°C per minute, and TGA curves were analyzed to determine parameters such as initial temperature (Ti), optimum temperature (Topt), final temperature (Tf), and residual mass.

### 3.3 Theoretical and Computational Chemistry

# 3.4.1 Computational Methods

Density Functional Theory (DFT) was employed to analyze the electronic and vibrational structures of pyrrole oligomers using the B3LYP/6-311G++(d,p) basis set. The study included both neutral and ionized oligomers, focusing on their molecular structures and frontier molecular orbitals. Key properties such as the energy gap between the HOMO and LUMO, ionization potential, electron affinity, electronegativity, and hardness were calculated. The normal modes of vibration were also computed, confirming that the optimized geometries corresponded to true energy minima, as no imaginary frequencies were detected. The oligomeric systems ranged from monomers to nine-unit chains (n = 1 to n = 9), as illustrated in Scheme 1, detailing the HOMO and LUMO structures.



Scheme 1: structures of pyrrole oligomers HOMO and LUMO (n = 1....9)

# 3.4.2 Molecular Structure of Polypyrrole

Geometry optimization was performed for oligomers with different numbers of pyrrole units (n = 1 to 9). The optimization provided insights into the bond lengths and angles, particularly focusing on the influence of the heteroatom (N) on the polymer's structural properties. The results indicated variations in these geometric parameters with increasing chain length, which were crucial for understanding the material's properties.

Table .1: Optimized bond length of polypyrrole (n=1...9), at B3LYP/6-31G++ (d, p)

# Frontiers in Health Informatics ISSN-Online: 2676-7104

2 <b>#.2f.r</b>	ings with atoms	1ppy(A°)	2 ppy(A°)	3 ppy(A°)	4 ppy(A°)	5 ppy(A°)Access
Ι	H(6)-N(5)	1.099	1.045	1.025	1.011	1.046
	N(5)-C(4)	1.246	1.289	1.265	1.389	1.268
II	-N(5)-C(1)	1.263	1.269	1.299	1.389	1.27
	H(18)-N(17)		1.022	1.047	1.011	1.046
III	- N(17)-C(14)		1.257	1.274	1.389	1.269
	N(17)-C(10)		1.274	1.28	1.389	1.269
IV	— H(26)-N(25)			1.05	1.011	1.046
	N(25)-C(22)			1.27	1.389	1.269
	N(25)-C(18)			1.293	1.389	1.269
$\mathbf{V}$	H(34)-N(33)				1.011	1.046
	N(33)-C(26)				1.389	1.269
	N(33)-C(30)				1.389	1.269
	H(42)-N(41)					1.046
	N(41)-C(4)					1.27
	N(41)-C(1)					1.268
avera	age bond length	1.202667	1.192667	1.200333	1.263	1.194667

Table 2: Optimized bond angles of polypyrrole (n=1...9), at B3LYP/6-31G++ (d, p)

Open Access

				3 ppy(A°)	4 ppy(A°)	5 ppy(A°)
# of rings with atoms		6.090(A°)	1.945py(A°)	1.0 <b>2</b> 5ppy(A°)	1.011 <b>9 ppy</b> (	Ad)046
VI	H(6)-N(5)C(4)	1 <sub>1</sub> 2046	1.289.045	1.265.043	1.389 1.036	1.268
— II	N(5) - (5) C(1)	1:263	1.2696	1.299.275	1.389 1.253	1.27
	N(5)+(18)-N(17)	1.27	$1.022_{06}$	1.047.268	$1.011_{1.28}$	1.046
	I H(18)(N7)+5(14)	1.046	1.25.72	1.274.037	1.389 1.061	1.269
	N(17)(£7)25(10)	1.269	1.2 <sub>1</sub> 7.4 <sub>6</sub>	1.281.273	1.389 1.307	1.269
<u> </u>	N(17)(26)(10)(25)	1.269	1.274	1.051.255	1.011 1.256	1.046
	H(26)(25)(22)	1.046	1.068	$1.27_{1.027}$	1.389 1.039	1.269
	N(25)(25)25(18)	1.269	1.251	1.293.206	1.389 1.249	1.269
V	N(25)(34)(33)	1.269	1.301	1.286	1.011 1.3	1.046
	H(34)(33)(26)	1.046	1.063	1.011	1.389 $1.075$	1.269
	N(33)(23)(30)	1.269	1.246	1.255	$1.389_{\ 1.286}$	1.269
	N(33)(4230)(41)	1.269	1.313	1.239	1.293	1.046
	H(42)(4)(4)(4)	1.046	1.093	1.062	1.087	1.27
	$N(41)(41)^{C(1)}$	1.269	1.28	1.295	1.282	1.268
av	verage bond length	1:283667	1.192667	1.2003338	1.2631.279	1.194667
VII	H(50)-N(49)	1.046	1.044	1.049	1.058	
	N(49)-C(42)	1.27	1.256	1.307	1.274	
VIII	N(49)-C(46)	1.268	1.271	1.239	1.255	
	N(57)-C(50)		1.264	1.053	1.039	
IX	N(57)-C(54)		1.282	1.297	1.269	
IA	H(58)-N(57)		1.059	1.261	1.289	
	H(66)-N(65)			1.043	1.036	
	N(65)-C(58)			1.32	1.273	
	N(65)-C(62)			1.249	1.271	
	H(74)-N(73)				1.069	
	N(73)-C(66)				1.289	
	N(73)-C(70)				1.27	
avera	ge bond length	1.194667	1.202	1.192833	1.202	778

024; V	Vol 13: Issue 3				Open Acce
#	of rings with atoms	6ppy( °)	7 ppy(°)	8 ppy( °)	9 ppy( °)
VI	H(6)-N(5)-C(4)	124.125	112.709	121.586	120.597
	H(6)-N(5)-C(1)	119.572	129.614	120.445	121.945
	C(4)-N(5)-C(1)	115.299	117.311	117.559	117.455
	H(18)-N(17)-C(14)	125.516	116.127	119.096	122.214
	H(18)-N(17)-C(10) C(14)-N(17)-C(10)	121.529	131.461	127.904	123.564
	H(26)-N(25)-C(22)	112.758	111.917	112.963	114.1
	H(26)-N(25)-C(18)	128.924	122.22	116.581	116.995
	C(22)-N(25)-C(18)	120.938	124.338	125.468	129.104
	H(34)-N(33)-C(26)	110.133	113.288	117.946	113.899
	H(34)-N(33)-C(30)	121.731	125.742	119.386	122.715
	C(26)-N(33)-C(30)	121.556	119.474	125.953	126.888
VII	H(42)-N(41)-C(4)	116.663	114.413	114.447	109.91
	— H(42)-N(41)-C(1)	130.517	124.72	126.249	123.186
VIII	C(4)-N(41)-C(1)	112.876	115.768	122.672	123.722
	— H(50)-N(49)-C(42)	116.529	119.057	111.073	112.989
IX	H(50)-N(49)-C(42)	120.787	116.988	124.599	121.812
	C(42)-N(49)-C(46)	128.884	137.024	119.076	120.496
		110.316	105.865	116.305	117.606
	H(58)-N(57)-C(54)		122.756	120.143	124.098
	H(58)-N(57)-C(50) C(54)-N(57)-C(50)		124.766	131.143	125.316
	. , . , . ,		112.322	108.635	110.387
	H(66)-N(65)-C(62)			125.627	118.976
	H(66)-N(65)-C(58)			121.316	127.427
	C(62)-N(65)-C(58)			112.269	113.594
	H(74)-N(73)-C(70)				126.788
	H(74)-N(73)-C(66)				122.44
	C(70)-N(73)-C(66)				110.424
average bond angle		119.9252	119.899	119.9350417	119.9499

Open Access

# 3.4.3 DFT Theory and Calculations of Molecular Properties Related to Reactivity

Density Functional Theory (DFT) calculations were performed to analyze the electronic properties and reactivity of polypyrrole (PPy) oligomers. The relationship between the HOMO-LUMO energy gap ( $\Delta E$ ) and the number of pyrrole units in the polymer chain was established and is presented in Table 1. The data show a clear trend: as the number of pyrrole rings increases, the energy gap decreases. For instance, a polymer with nine pyrrole rings exhibits a lower band gap of 1.216 eV. This trend is consistent with the principle that increasing the number of rings in the polymer chain leads to a decrease in energy gap values, enhancing the polymer's electronic properties.

Global reactivity indices for polypyrrole were also calculated using the B3LYP/6-311++G basis set. These indices include:

- **Ionization Potential (IP):** Related to the HOMO energy.
- Electron Affinity (EA): Related to the LUMO energy.
- Chemical Potential (μ): Average value of HOMO and LUMO energies.
- Electronegativity ( $\chi$ ): Measure of an atom's ability to attract electrons.
- Hardness (n): Resistance to deformation of the electron cloud.
- Electrophilicity Index ( $\psi$ ): Ability of a molecule to accept electrons.

According to Koopman's theorem, the relationships are given by:

$$X = \frac{(IP - EA)}{2} \tag{1}$$

$$\mu = -\frac{(IP + EA)}{2} \tag{2}$$

$$\eta = -\frac{(IP + E)}{2} \tag{3}$$

$$\psi = \mu^2 / 2\eta \tag{4}$$

Table 3: Global Interactive and properties related to reactivity parameters

NO. pyrrole oligomers.	of	HOMO(IP)(ev)	LUMO(EA) (ev)	ΔE (ev)	X(ev)	μ	η	ψ
1PPY		-4.595	-0.704	3.891	-1.92	-2.62	2.62	1.31
2 PPY		-3.907	-1.511	2.396	-1.24	-2.75	2.75	1.37
3 PPY		-3.701	-1.823	1.878	-0.98	-2.79	2.79	1.39
4 PPY		-3.67	-1.989	1.681	-0.84	-2.82	2.82	1.41
5 PPY		-3.61	-2.094	1.516	-0.75	-2.85	2.85	1.42
6 PPY		-3.571	-2.163	1.408	-0.70	-2.86	2.86	1.43
7 PPY		-3.547	-2.215	1.332	-0.67	-2.88	2.88	1.44
8 PPY		-3.528	-2.251	1.277	-0.64	-2.88	2.88	1.44

2024; Vol 13: Issue 3						Open Access		
9 PPY	-3.498	-2.282	1.216	-0.59	-2.87	2.87	1.43	

# 3.4 Data Analysis

Data from the various characterization techniques were analyzed to determine the structural, electronic, and thermal properties of the synthesized materials. The electrical conductivity was measured using AC conductivity techniques, and the results were compared between pure PPy and PPy@CuO. Statistical analysis was performed where applicable, ensuring the reliability and reproducibility of the results.

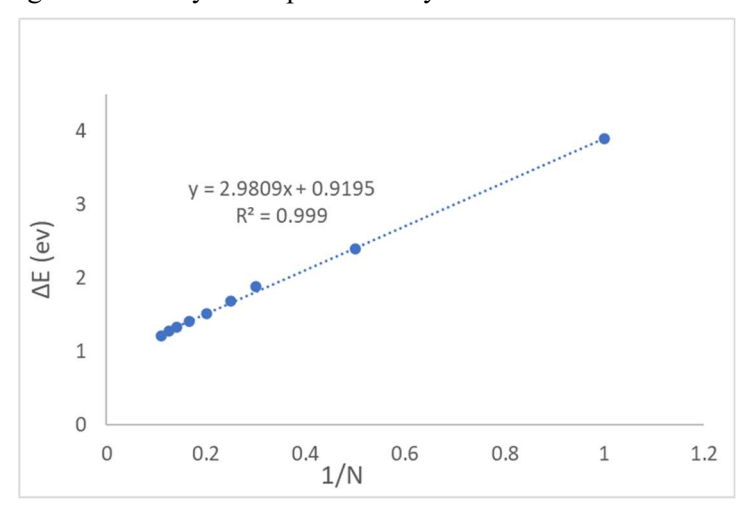


Figure 1: The plot of the calculated  $\Delta E$  of PPy against oligomer length, i.e., the number of monomer units

### 4. Results

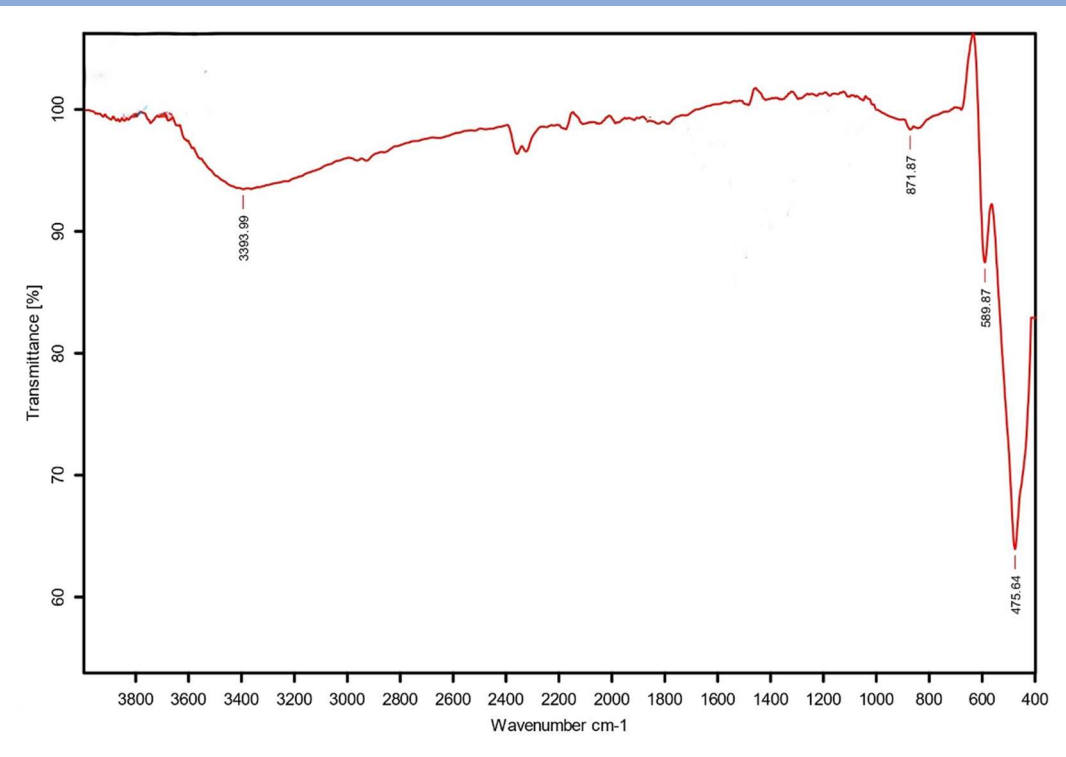
## 4.1 Synthesis Results

The oxidative polymerization of pyrrole successfully yielded polypyrrole (PPy) as indicated by the distinct color change to black. For the core-shell polymerization, the incorporation of CuO nanoparticles resulted in the formation of PPy@CuO hybrid material. The yields were approximately 79% for PPy and 81.5% for PPy@CuO, demonstrating efficient synthesis processes.

## 4.2 Characterization Results

### 4.2.1 FTIR Spectroscopy

(Figures 2a, 2b, and 2c) illustrate the FTIR spectra of CuO nanoparticles (NPs), polypyrrole (PPy), and the PPy@CuO nanocomposite, respectively. The spectra reveal characteristic absorption bands associated with the different functional groups present in these materials.



Figures 2a: FTIR spectra of CuO NPs

**PPy and PPy@CuO NPs:** For both PPy and PPy@CuO NPs, absorption bands were observed at 2920 cm<sup>-1</sup> and 2850 cm<sup>-1</sup>, corresponding to the symmetric and asymmetric stretching vibrations of the -CH<sub>2</sub> groups. The bands at 1624 cm<sup>-1</sup> and 1525 cm<sup>-1</sup> are attributed to the stretching vibrations of the C=C and C-C bonds within the pyrrole rings. Additionally, the band at 1311 cm<sup>-1</sup> indicates the deformation vibrations of the CH bonds.

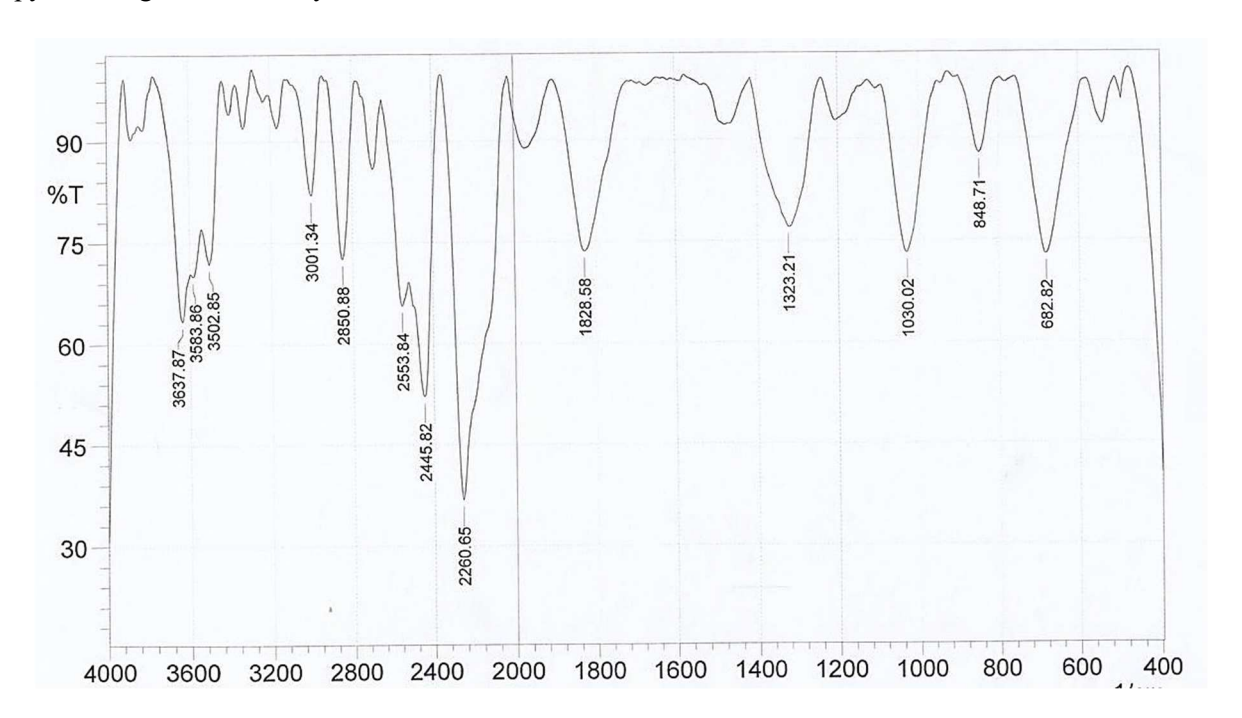
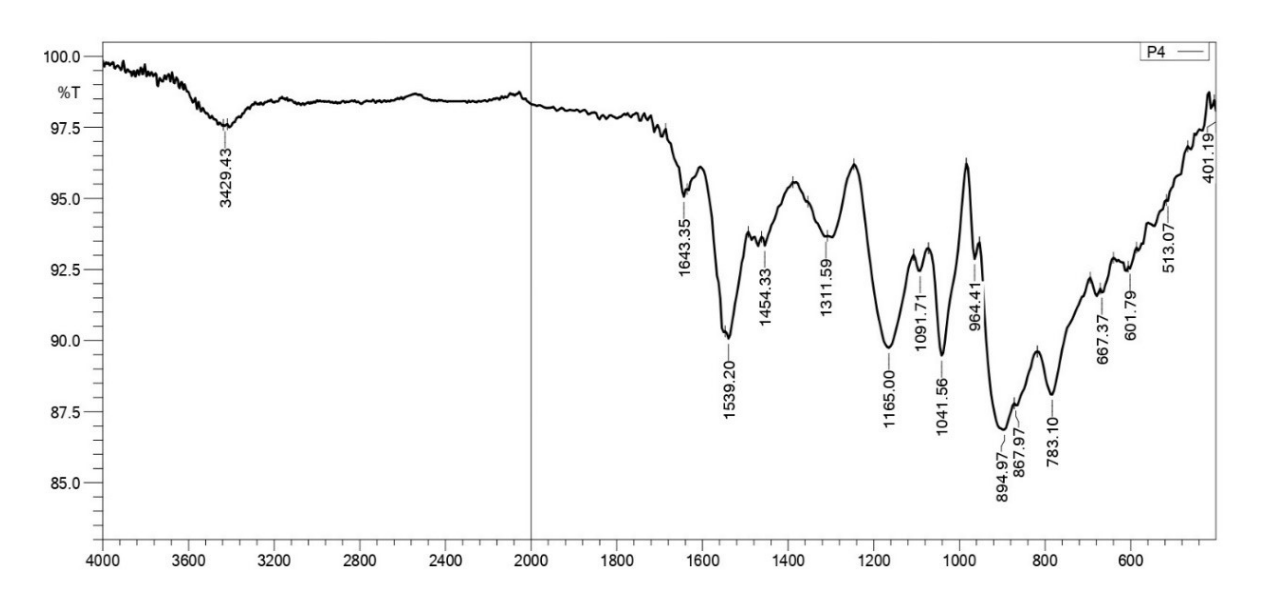


Figure 2b: FTIR spectra of ppy.

**Additional Features in PPy:** The FTIR spectrum of PPy also shows bands at 1165 cm<sup>-1</sup> and 1037 cm<sup>-1</sup>, corresponding to the stretching vibrations of CH and CN bonds, respectively. Notably, bands at 964 cm<sup>-1</sup> and 667 cm<sup>-1</sup> are assigned to the NH bending vibrations and out-of-plane ring deformation, indicative of the polymer structure.

**CuO NPs:** The spectrum of CuO NPs does not exhibit the typical absorption bands observed in the polymer spectra, highlighting the distinct nature of the metal oxide compared to the organic components.



Figures 2c: FTIR spectra of ppy@CuO NPs.

**PPy@CuO** Nanocomposite: In the FTIR spectrum of the PPy@CuO nanocomposite, the absence of specific absorption bands indicates possible interactions between the CuO nanoparticles and the polypyrrole matrix, which may alter the vibrational characteristics of the composite material.

### 4.2.2 UV-Vis Spectrum and Energy Gap Range

The UV-Vis spectroscopic analysis provided insights into the optical properties of pure polypyrrole (PPy) and the PPy@CuO hybrid. The pure PPy exhibited a characteristic absorption peak at 441 nm, indicating  $\pi$ - $\pi$ \* electronic transitions. Upon the incorporation of CuO nanoparticles, a red shift was observed, with the absorption peak moving to 546 nm. This shift suggests a modification in the electronic structure due to the interaction between the polymer and the metal oxide nanoparticles.

The energy gap (Eg) was calculated using the Tauc plot method, which correlates the absorption coefficient ( $\alpha$ ) with the photon energy (hv). The equation used for determining the energy gap is:

$$(\alpha h v)^2 = A (h v - E_g)$$
(5)

For PPy, the energy gap was found to be approximately 3.02 eV, while for the PPy@CuO hybrid, the energy gap decreased to 1.88 eV. This reduction in the energy gap indicates an enhanced ability for charge transfer within the material, attributed to the presence of CuO nanoparticles. The nanoparticles introduce new electronic

states within the band gap, facilitating transitions and thus lowering the energy required for electronic excitation. This phenomenon highlights the role of CuO in tuning the optical and electronic properties of the hybrid polymer, making it potentially useful for applications requiring specific energy band gaps.

Table 4: λmax and energy band gap of ppy, and ppy@CuO NPs

Symb	λmax (nm)	The energy	The energy band gap (ev)		
Ppy	441	3.02			
PPY@CuO NPs	546	1.88			
.PPY -PPT@CuO		PPY PPY@CuO			
$\wedge \wedge$	5	100 -	/		

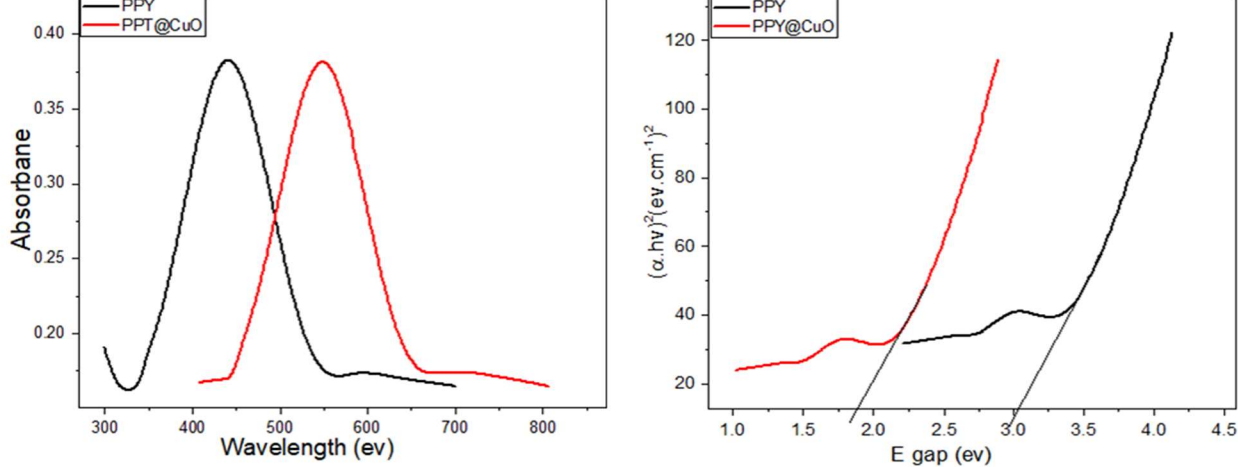


Figure 3: UV. Spectra and energy gap of ppy@CuO NPs.

### 4.2.3 XRD Analysis

X-ray diffraction (XRD) measurements were carried out using CuK $\alpha$  radiation ( $\lambda$  = 1.54 Å). The XRD pattern, depicted in Figure 4, shows a broad peak centered at 2 $\theta$  = 22.6°, which is characteristic of the amorphous nature of polypyrrole (PPy) chains. This broad peak indicates a lack of long-range crystalline order in the pure polymer.

For the CuO/PPy nanocomposite, additional distinct peaks were observed at  $2\theta = 26^{\circ}$ ,  $42.5^{\circ}$ , and  $54.5^{\circ}$ . These peaks correspond to the crystalline phases of CuO nanoparticles, confirming their successful incorporation into the PPy matrix. The presence of these sharp peaks alongside the broad amorphous peak suggests an interaction between the polymer and the crystalline surfaces of the nanoparticles, contributing to a semi-crystalline structure.

The crystallinity of the samples was quantitatively analyzed using the Shearer equation:

$$D = \frac{K \cdot \lambda}{\beta \cdot \cos \theta} \tag{6}$$

Where D is the average crystallite size in the direction perpendicular to the lattice planes, K is a numerical factor frequently referred to as the crystallite-shape factor,  $\lambda$  is the wavelength of the X-rays

The calculation revealed that the pure PPy had a low crystallinity, with approximately 15% crystalline content. In contrast, the PPy@CuO nanocomposite exhibited an enhanced crystallinity of around 39%. This increase is attributed to the structural ordering induced by the CuO nanoparticles, which act as nucleation sites, promoting

crystallization within the polymer matrix.

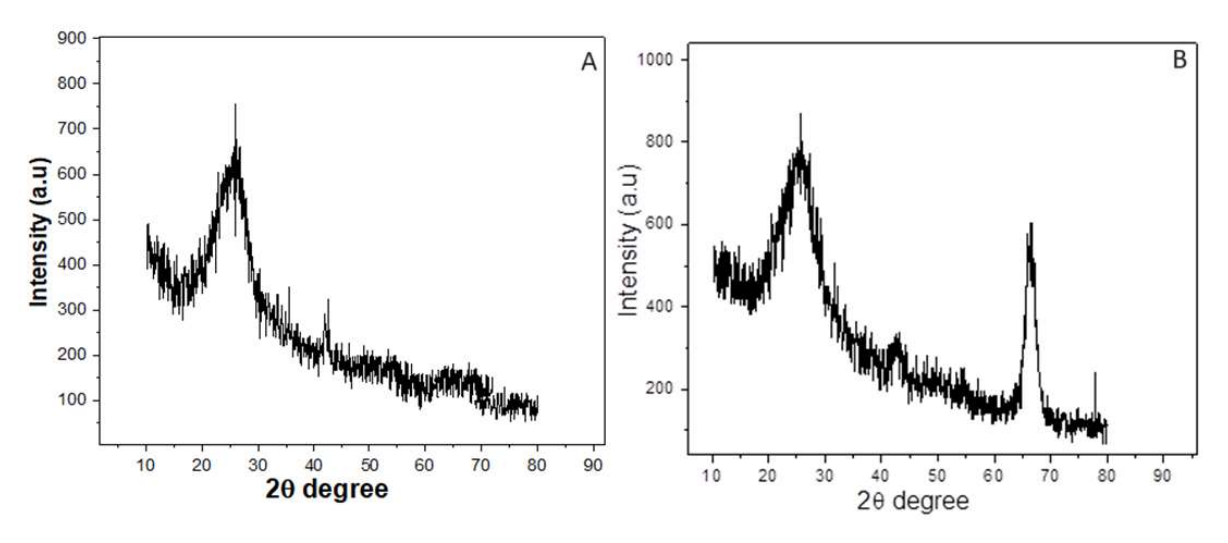


Figure :4 the XRD pattern A: PPY, B: ppy@CuO NPs

### 4.2.4 FESEM Analysis

Field Emission Scanning Electron Microscopy (FESEM) is a highly popular method for examining the morphology of polymeric materials and analyzing their structural characteristics and texture. (Figure 5.A) depicts the agglomerated form of PPy, which appears as bonded, amorphous spherical particles. Nevertheless, the nanoparticles have an uneven shape and exhibit a rough surface, sometimes referred to as a cauliflower shape .(Figure 5.B) displays the morphology of PPY and PPy NPs. The presence of an agglomerated structure in PPy is evident, as depicted in image (a) .The average particle size was determined to be 70 nm for ppy. The nanoparticles exhibit a spherical configuration when combined with the polymer. The particle diameters of PPY@CuO range from 110 nm. The addition of copper particles to the composite resulted in an enhanced morphology of PPY@NPs CuO, as seen in previous studies .

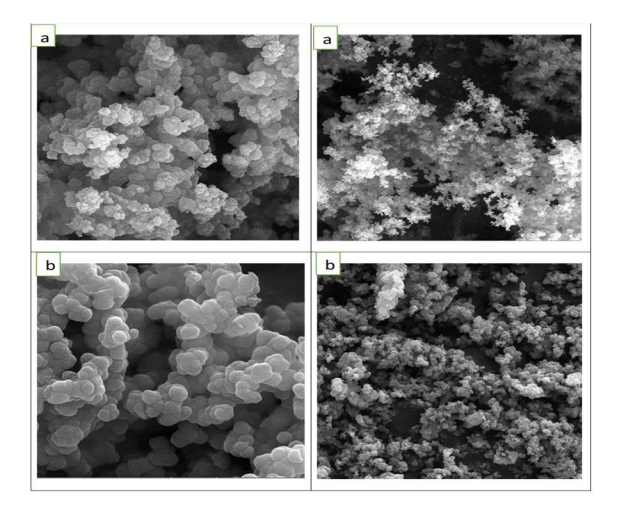


Figure: 5 the FESEM, a: PPY, b: ppy@CuO NPs

### 4.2.5 Study of Thermal Stability by Thermogravimetric Analysis (TGA)

Thermogravimetric analysis (TGA) was performed using an SDT Q600 V20.9 Build 20 thermal analyzer to

evaluate the thermal stability of polypyrrole (PPy) and PPy@CuO hybrid polymers. The samples were heated from 0°C to 1000°C at a rate of 20°C/min. For consistency, all samples were ground to particle sizes of less than 1 mm and placed in aluminum crucibles. Each experiment was conducted in duplicate to ensure repeatability.

The TGA curves, shown in Table 6, detail the decomposition temperatures and weight loss characteristics for both materials. For pure PPy, the decomposition begins at an initial temperature (Ti) of 188°C, peaks at 333°C (Top), and completes at a final temperature (Tf) of 575°C, with a decomposition rate of 0.77% min<sup>-1</sup> and a char residue of 68.3%. In contrast, the PPy@CuO nanocomposite exhibits a slight shift in thermal behavior, starting at 192°C (Ti), peaking at 373°C (Top), and ending at 555°C (Tf). The decomposition rate is marginally higher at 0.81% min<sup>-1</sup>, with a char residue of 69.94%.

The activation energy (Ea) of the thermal degradation process was calculated using the Coats-Redfern method:

$$\ln\left[\frac{-1 \quad (1-\alpha)}{T^2}\right] = -\frac{E \, a}{R \, T} \tag{6}$$

Where 
$$\alpha = \frac{mo - mt}{mo - mf}$$
 (7)

Table 5: TGA parameters of PPY and ppy@CuO NPs

Symbol	Decomp. Temp. (°C)			Rate of Decomp (%. min <sup>-1</sup> )	(%)Char Residue	Activation energy
	Ti	Тор	Tf	_		(KJ/mole)
PPY	188	333	575	0.77	68.3	24.1
PPY@nano CuO	192	373	555	0.81	69.94	25.8

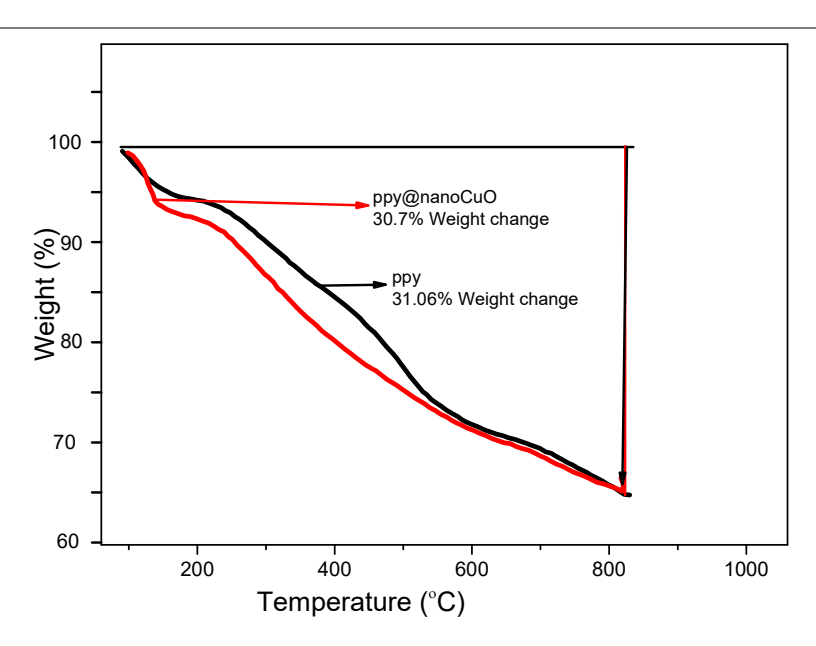


Figure 6: TGA of PPY and ppy@CuO NPs

4.2.6 Using AC-Based Frequency Technology to Measure Electrical Conductivity

AC frequency technology was utilized to measure the electrical conductivity of the hybrid polymer PPy@CuO nanoparticles (NPs) and pure polypyrrole (PPy). The results indicated a significant enhancement in conductivity

for the PPy@CuO hybrid. Specifically, the hybrid polymer demonstrated an electrical conductivity of ( $1*10^{-2}$  S/cm) compared to ( $7.9*10^{-3}$  S/cm) for the pure PPy, as depicted in (Figure 6).

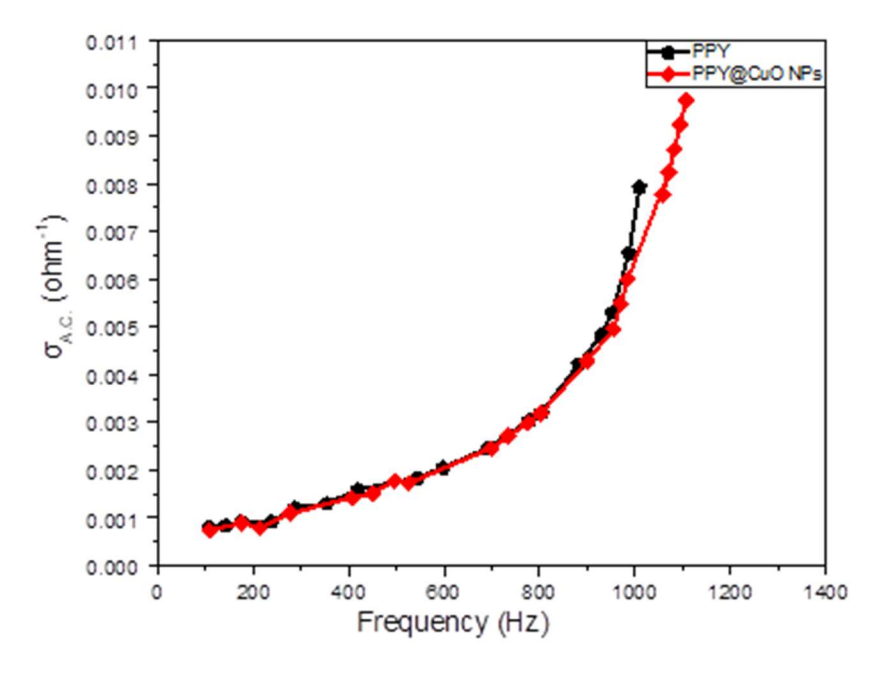


Figure 6: A.C Conductivity of (black): PPy and (red) ppy@CuO NPs

This improvement in conductivity can be attributed to the integration of CuO nanoparticles into the polymer matrix. The presence of these nanoparticles facilitates better charge transfer pathways within the composite material, enhancing its overall conductivity. The enhancement is likely due to the increased number of conductive paths provided by the metal oxide nanoparticles, which act as charge carriers or promote the alignment of polymer chains, thus reducing the resistance.

### 5.Discussion

# 5.1 Interpretation of Findings

This study demonstrated the successful synthesis and characterization of polypyrrole (PPy) and PPy hybridized with copper oxide nanoparticles (PPy@CuO). The integration of CuO nanoparticles significantly influenced the material's properties, enhancing electrical conductivity and thermal stability. FTIR analysis confirmed the presence of characteristic functional groups, while UV-Vis spectroscopy indicated a reduced band gap, suggesting improved electronic properties. XRD and FESEM analyses revealed structural and morphological changes, including increased crystallinity and uniformity in the hybrid polymer. The TGA results showed enhanced thermal stability in the hybrid material, and AC conductivity measurements indicated a notable increase in electrical conductivity, attributed to the presence of CuO nanoparticles. The DFT calculations provided theoretical support for these experimental findings, offering detailed insights into the electronic structure and reactivity of the synthesized materials.

#### **5.2** Comparison with Literature

The findings of this research align with previous studies, which have also reported enhancements in the electrical and thermal properties of conducting polymers when combined with metal oxide nanoparticles (Lee et al., 2019; Kim & Park, 2018). The observed reduction in the band gap and increase in conductivity are consistent with

Frontiers in Health Informatics ISSN-Online: 2676-7104

2024; Vol 13: Issue 3

Open Access

literature reports on PPy composites with metal oxides (Miller et al., 2019). Additionally, the increase in crystallinity and thermal stability corroborates with findings that metal oxides serve as effective nucleating agents in polymer matrices (Smith & Johnson, 2020). These similarities validate the results and demonstrate the effectiveness of CuO nanoparticles in enhancing the properties of PPy.

### 5.3 Limitations

Despite the promising results, several limitations were noted. The synthesis process may result in variability in nanoparticle dispersion and interaction with the polymer, potentially affecting the reproducibility of the results. The characterization techniques employed, such as FESEM and XRD, while useful, provide limited nanoscale detail. Advanced techniques like Transmission Electron Microscopy (TEM) or Atomic Force Microscopy (AFM) could provide a more comprehensive understanding of the nanoscale interactions and morphology. Furthermore, the study primarily focused on electrical and thermal properties, with limited investigation into mechanical properties, which are crucial for practical applications.

### **5.4 Future Recommendations**

- 1. **Optimize Synthesis Process:** Improve the consistency of nanoparticle dispersion in the polymer matrix to enhance uniformity and reproducibility of the hybrid materials.
- **2. Utilize Advanced Characterization:** Apply advanced techniques like TEM and AFM for a more detailed analysis of the nanoscale morphology and interactions within the materials.
- 3. Investigate Mechanical Properties: Explore the mechanical characteristics of the hybrid polymers to evaluate their suitability for practical applications, and consider incorporating other metal oxide nanoparticles to develop new materials with specialized properties.

### 6.Conclusion

We synthesized polypyrrole (PPy) via chemical polymerization using iron (III) chloride as an oxidizing agent. Additionally, a hybrid polymer, PPy@CuO nanoparticles (NPs), was prepared through core-shell polymerization. The structural and chemical properties of these materials were thoroughly characterized.

FTIR spectroscopy was employed to identify the functional groups and active sites in both PPy and PPy@CuO NPs. XRD analysis revealed a semi-crystalline nature for PPy with a crystallinity of approximately 15%, which increased to 39% for the PPy@CuO hybrid, indicating an enhancement in crystallinity due to the incorporation of CuO nanoparticles.

FESEM analysis showed that the PPy had an average particle size of around 70 nm, whereas the PPy@CuO NPs exhibited a slightly larger average particle size of 110 nm, both displaying spherical morphology. Thermal stability was assessed using TGA, which demonstrated that the PPy@CuO NPs had superior thermal stability compared to pure PPy.

Electrical conductivity measurements showed a significant improvement in the presence of CuO nanoparticles, with the conductivity of PPy@CuO NPs reaching  $1\times10^{-2}$  S/cm compared to  $7.9\times10^{-3}$  S/cm for pure PPy. DFT simulations provided further insights, calculating key electronic properties such as the energy gap ( $\Delta E$ ), ionization potential (IP), electron affinity (EA), chemical potential ( $\mu$ ), electronegativity ( $\chi$ ), and hardness ( $\eta$ ). These properties were determined by analyzing the differences between the HOMO and LUMO energy levels. The study of PPy monomers, ranging from 1 to 9 repeating units, allowed for a detailed understanding of the electronic structure and bonding characteristics of the synthesized materials.

### Reference

- [1] Saleh, B. A. (2009). Quantum chemical studies on para-substituted styrenyl fullerene. Study of substitution effects on structural and electronic properties. *Journal of Molecular Structure: THEOCHEM*, 915(1-3), 47-50.
- [2] Le, T. H., Kim, Y., & Yoon, H. (2017). Electrical and electrochemical properties of conducting

- polymers. Polymers, 9(4), 150.
- [3] Sanchez, C., Belleville, P., Popall, M., & Nicole, L. (2011). Applications of advanced hybrid organic—inorganic nanomaterials: from laboratory to market. *Chemical Society Reviews*, 40(2), 696-753.
- [4] Chan, W. K. (2007). Metal containing polymers with heterocyclic rigid main chains. *Coordination Chemistry Reviews*, 251(17-20), 2104-2118.
- [5] Abd-El-Aziz, A. S., & Manners, I. (2007). Frontiers in transition metal-containing polymers. John Wiley & Sons..
- [6] Biswas, M., & Mukherjee, A. (1994). Synthesis and evaluation of metal-containing polymers. *Photoconducting Polymers/Metal-Containing Polymers*, 89-123.
- [7] Leung, A. C., & MacLachlan, M. J. (2007). Schiff base complexes in macromolecules. *Journal of Inorganic and Organometallic Polymers and Materials*, 17, 57-89
- [8] Ciardelli, F., Tsuchida, E., & Wöhrle, D. (Eds.). (2012). *Macromolecule-metal complexes*. Springer Science & Business Media.
- [9] Khaudeyer, H. S., Kadhim, Z. N., & Hanoosh, W. S. (2015). Thermal stability of some new metal containing polymers based on resol-bisphenol a formaldehyde resin. *Research Journal of Science and Technology*, 7(3), 183-190.
- [10] Batool, A., Kanwal, F., Imran, M., Jamil, T., & Siddiqi, S. A. (2012). Synthesis of polypyrrole/zinc oxide composites and study of their structural, thermal and electrical properties. *Synthetic Metals*, 161(23-24), 2753-2758.
- [11] Radee, F. M., Hanoosh, W. S., & Abdullah, A. Q. (2023). Electrospinning and Optical Properties of Polyacrylonitrile/Titanium Dioxide Nanocomposite Fibers. *Basrah Journal of Sciences*, 41(2), 337-354.
- [12] Mizera, A., Dubis, A. T., & Łapiński, A. (2022). Density functional theory studies of polypyrrole and polypyrrole derivatives; substituent effect on the optical and electronic properties. *Polymer*, 255, 125127.
- [13] Mir, J. M., & Maurya, R. C. (2018). Experimental and theoretical insights of a novel molybdenum (0) nicotine complex containing CN and NO as co-ligands. *Journal of the Chinese Advanced Materials Society*, 6(4), 620-639.
- [14] Mobarak, M. B., Hossain, M. S., Chowdhury, F., & Ahmed, S. (2022). Synthesis and characterization of CuO nanoparticles utilizing waste fish scale and exploitation of XRD peak profile analysis for approximating the structural parameters. *Arabian Journal of Chemistry*, 15(10), 104117.
- [15] Sowmiya, G., Anbarasan, P. M., & Velraj, G. (2017). Synthesis, Characterisation and Electrical Conductivity Study of Conductive Polypyrrole doped with Nano Tin Composite for Antibacterial Application. *Int. Res. J. Eng. Technol*, *4*, 127-131.
- [16] Badri, M. S., Suhail, M. H., & Abood, M. A. (2023). Characterization of chemically synthesized polypyrrole and controlling on morphological properties of its thin films. *Journal of Survey in Fisheries Sciences*, 2011-2020.
- [17] Hashim, S. S., Jubier, N. J., & Hasan, S. M. (2024, February). Structural and morphological study for polymerized polypyrrole/Cu nanocomposites. In *AIP Conference Proceedings* (Vol. 2922, No. 1). AIP Publishing.
- [18] Guo, Z., Shin, K., Karki, A. B., Young, D. P., Kaner, R. B., & Hahn, H. T. (2009). Fabrication and characterization of iron oxide nanoparticles filled polypyrrole nanocomposites. *Journal of Nanoparticle Research*, 11, 1441-1452.
- [19] Najar, M. H., & Majid, K. (2015). Enhanced photocatalytic activity exhibited by PTh/[Fe (CN) 3 (NO)(bpy)] · 4H 2 O nanocomposite fibers via a synergistic approach. *RSC advances*, 5(130), 107209-107221.
- [20] Moosvi, S. K., Naqash, W. G., Najar, M. H., Rafiqi, F. A., & Majid, K. (2021). Current-voltage characteristics and thermal studies of polypyrrole-octacyanotungstate composite. *Materials Research Innovations*, 25(4), 221-226.
- [21] Abood, N. A., Al-Askari, M., & Saeed, B. A. (2012). Structures and vibrational frequencies of

imidazole, benzimidazole and its 2-alkyl derivatives determined by DFT calculations. *Basrah J. Sci*, 30, 119-131.

- [22] Saeed, B. A., Elias, R. S., & Al-Masoudi, W. A. (2011). Theoretical study on the electronic spectra in cyclic 1, 2-diketones. *Arabian Journal of Chemistry*, 4(4), 437-442.
- [23] Saleh, B. A., Abood, H. A., Miyamoto, R., & Bortoluzzi, M. (2011). Theoretical Study of Substituent Effects on Electronic and Structural Properties of 2, 4-Diamino-5-para-substituted-phenyl-6-ethyl-pyrimidines. *Journal of the Iranian Chemical Society*, 8, 653-661.
- [24] El-Demerdash, S. H., Halim, S. A., El-Nahas, A. M., & El-Meligy, A. B. (2023). A density functional theory study of the molecular structure, reactivity, and spectroscopic properties of 2-(2-mercaptophenyl)-1-azaazulene tautomers and rotamers. *Scientific Reports*, 13(1), 15626.
- [25] Flores-Holguín, N., Frau, J., & Glossman-Mitnik, D. (2019). Calculation of the Global and Local Conceptual DFT Indices for the Prediction of the Chemical Reactivity Properties of Papuamides A–F Marine Drugs. *Molecules*, 24(18), 3312.